Article:

Mifsud, J. and van de Bruck, C. (2019) An interacting dark sector and the implications of the first gravitational-wave standard siren detection on current constraints. Monthly Notices of the Royal Astronomical Society, 487 (1). pp. 900-907. ISSN 0035-8711

https://doi.org/10.1093/mnras/stz1293

Monthly Notices
of the
ROYAL ASTRONOMICAL SOCIETY

MNRAS **487,** 900–907 (2019)
Advance Access publication 2019 May 22

doi:10.1093/mnras/stz1293

An interacting dark sector and the implications of the first gravitational-wave standard siren detection on current constraints

Jurgen Mifsud★ and Carsten van de Bruck

Consortium for Fundamental Physics, School of Mathematics and Statistics, University of Sheffield, Hounsfield Road, Sheffield S3 7RH, UK

Accepted 2019 April 28. Received 2019 April 13; in original form 2019 February 10

ABSTRACT

After the first nearly simultaneous joint observations of gravitational waves and electromagnetic emission produced by the coalescence of a binary neutron star system, another probe of the cosmic expansion, which is independent from the cosmic distance ladder, became available. We perform a global analysis in order to constrain an interacting dark energy model, characterized by a conformal interaction between dark matter and dark energy, by combining current data from: *Planck* observations of the cosmic microwave background radiation anisotropies, and a compilation of Hubble parameter measurements estimated from the cosmic chronometers approach as well as from baryon acoustic oscillation measurements. Moreover, we consider two measurements of the expansion rate of the Universe today, one from the observations of the Cepheid variables, and another from the merger of the binary neutron star system GW170817. We find that in this interacting dark energy model, the influence of the local measurement of the Hubble constant mostly affects the inferred constraints on the coupling strength parameter between dark energy and dark matter. However, the GW170817 Hubble constant measurement is found to be more conservative than the Cepheid variables measurement, and in a better agreement with the current high-redshift cosmological data sets. Thus, forthcoming gravitational-wave standard siren measurements of the Hubble constant would be paramount for our understanding of the dark cosmic sector.

Key words: gravitational waves – cosmological parameters – dark energy – dark matter.

1 INTRODUCTION

Gravitational-wave multimessenger astronomy paved the way for the possibility of using standard sirens to infer the current expansion rate of our Universe. It has long been acknowledged (see for instance, Schutz 1986; Krolak & Schutz 1987; Chernoff & Finn 1993; Markovic 1993; Finn 1996; Thorne 1997; Wang & Turner 1997; Zhu, Fujimoto & Tatsumi 2001; Holz & Hughes 2005; Dalal et al. 2006; Taylor, Gair & Mandel 2012; Nissanke et al. 2013) that gravitational-wave inspiral detections would provide us with invaluable cosmological information. Since the amplitude of a binary's gravitational-wave signal encodes its luminosity distance (Congedo 2017), binary inspirals became known as standard sirens (Schutz 1986), which are the gravitational-wave analogues of type Ia supernovae standard candle measurements. In particular, the determination of the Hubble constant from gravitational-wave standard sirens (Schutz 1986; Krolak & Schutz 1987; Chernoff & Finn 1993; Finn 1996; Dalal et al. 2006; Taylor et al. 2012; Nissanke et al. 2013) was demonstrated for the first time by the nearly concurrent joint observations of the electromagnetic counterpart (see Abbott et al. 2017c,d; Arcavi et al. 2017; Coulter et al. 2017; Goldstein et al. 2017; Savchenko et al. 2017; Soares-Santos et al. 2017; Valenti et al. 2017; Tanvir et al. 2017, and references therein) to the gravitational-wave signal (Abbott et al. 2017a) produced by the merger of the binary neutron star system GW170817 that has been localized to the host galaxy NGC 4993.

Although the first constraint on the Hubble constant from standard sirens (Abbott et al. 2017b) is significantly weaker than the inferred constraints from observations of Cepheid variables [see Riess et al. (2016), and the new analysis of Riess et al. (2018a,b)] and the extrapolated concordance model cosmic microwave background (CMB) measurement (Aghanim et al. 2016b) (see also Ade et al. 2014a, 2016a; Aghanim et al. 2018), prospective gravitational-wave standard siren measurements of the Hubble constant are expected to be significantly improved after the detection of additional standard siren events. Consequently, these near-future standard siren measurements of the Hubble constant would be competitive with the measurements inferred from the more established methods (Chen, Fishbach & Holz 2018; Feeney et al. 2018a; Hotokezaka et al. 2018). Moreover, standard siren measurements of the Hubble constant are independent of the cosmic distance ladder or poorly understood calibration processes, as these are primarily calibrated

★ E-mail: jmifsud1@sheffield.ac.uk

by the robust theory of General Relativity to cosmological scales and instrumental systematics are expected to be inconsequential (Karki et al. 2016; Cahillane et al. 2017; Davis et al. 2019). Furthermore, we should also point out that the reported standard siren constraint of $H_0 = 70^{+12}_{-8}$ km s^{-1} Mpc^{-1} at the 68 per cent confidence level is strongly non-Gaussian (Abbott et al. 2017b), with the major uncertainty being the inclination plane of the binary orbit. This independent probe of the present-day cosmic expansion is paramount for the reported discrepancy at the ($\gtrsim$)3σ level (Feeney, Mortlock & Dalmasso 2018b) between the locally measured (Riess et al. 2016) and the CMB-derived estimate (Aghanim et al. 2016b) of the Hubble constant, as forthcoming standard siren detections would be able to adjudicate between these discrepant measurements (Feeney et al. 2018a). Such disagreement could either be an indication of several physical mechanisms beyond our concordance model of cosmology (see for instance, Bernal, Verde & Riess 2016; Di Valentino, Melchiorri & Silk 2016; Grandis et al. 2016; Huang & Wang 2016; Karwal & Kamionkowski 2016; Odderskov, Baldi & Amendola 2016; Di Valentino, Melchiorri & Mena 2017b; Lancaster et al. 2017; Prilepina & Tsai 2017; Solá, Gómez-Valent & de Cruz Pérez 2017; Zhao et al. 2017b; Colgáin, Van Putten & Yavartanoo 2018; Di Valentino, Linder & Melchiorri 2018b; Poulin et al. 2018; van de Bruck & Mifsud 2018), or unidentified systematic errors (see Addison et al. 2016; Cardona, Kunz & Pettorino 2017; Odderskov, Hannestad & Brandbyge 2017; Wu & Huterer 2017; Zhang et al. 2017; Dhawan, Jha & Leibundgut 2018; Feeney et al. 2018b; Follin & Knox 2018; Camarena & Marra 2018, and references therein), although there is still no compelling explanation to date.

Given that the derived Hubble constant measurement from the CMB assumes a Lambda cold dark matter (ΛCDM) cosmic evolution, in which the cosmological expansion is dominated by a cosmological constant (Λ) and cold dark matter (CDM), a number of alternative cosmological models have been proposed. For instance, models with a time-evolving (Zhao et al. 2017a; Di Valentino et al. 2018b) along with other non-standard dark energy cosmic components (Huang & Wang 2016; Karwal & Kamionkowski 2016; Di Valentino et al. 2017a,b; Yang et al. 2018, 2019), and neutrino contributions (Archidiacono et al. 2016; Ko & Tang 2016; Kumar & Nunes 2016; Riess et al. 2016; Yang et al. 2017; Zhao et al. 2017b; Benetti, Graef & Alcaniz 2018; Di Valentino et al. 2018a) have been shown to partially alleviate this Hubble constant tension reported in the ΛCDM framework. Thus, independent gravitational-wave standard siren measurements of the Hubble constant would certainly shed light on the physics beyond the concordance cosmological model, particularly when the sub-per cent level is attained. Such accurate standard siren measurements have repeatedly shown that these will be able to constrain the cosmological parameters (see for instance, Dalal et al. 2006; MacLeod & Hogan 2008; Cutler & Holz 2009; Sathyaprakash, Schutz & Van Den Broeck 2010; Zhao et al. 2011; Del Pozzo 2012; Nishizawa et al. 2012; Taylor & Gair 2012; Tamanini et al. 2016; Belgacem et al. 2018; Di Valentino et al. 2018c; Feeney et al. 2018a; Congedo & Taylor 2019), and would be of utmost importance for the forthcoming CMB and baryon acoustic oscillation (BAO) surveys that are expected to reach an unprecedented level of accuracy (Abazajian et al. 2016; Di Valentino et al. 2018d).

We should also remark that apart from the Hubble constant measurement, the observations of gravitational wave and electromagnetic emission from the coalescence of the binary neutron star system GW170817 have been used to test our understanding of gravitation and astrophysics (Lombriser & Taylor 2016; Abbott et al. 2017d, 2018). For instance, the fractional speed difference between the speed of light and that of gravity has been exquisitely found to be less than about one part in 10^{15} (Abbott et al. 2017d), which consequently led to stringent constraints on several modified theories of gravity (see for instance, Baker et al. 2017; Creminelli & Vernizzi 2017; Ezquiaga & Zumalacárregui 2017; Sakstein & Jain 2017; de Rham & Melville 2018; Dima & Vernizzi 2018; Langlois et al. 2018).

It is therefore timely to investigate the impact of the first gravitational-wave standard siren measurement of the Hubble constant on the current CMB and cosmic expansion constraints in the framework of a cosmological model characterized by a non-standard interacting dark sector. A similar analysis has been carried out in an extended ΛCDM model (Di Valentino & Melchiorri 2018), in which the inclusion of the GW170817 Hubble constant measurement led to improved constraints on the model parameters. We here consider a cosmological model in which dark matter and dark energy interact with one another, whereas the standard model (SM) particles follow their standard cosmological evolution. Consequently, this coupled dark energy model evades the tight constraints inferred from the equivalence principle and Solar system tests (Bertotti, Iess & Tortora 2003; Will 2014). Due to the obscure nature of dark matter and dark energy, a dark sector coupling cannot be excluded from the viewpoint of fundamental physics (Damour, Gibbons & Gundlach 1990; Wetterich 1995; Carroll 1998; Holden & Wands 2000; Farrar & Peebles 2004; Gubser & Peebles 2004; Carroll et al. 2009), and such an interaction between these dark sector constituents is not currently forbidden by cosmological data (see for instance, Salvatelli et al. 2014; Kumar & Nunes 2016, 2017; Ferreira et al. 2017; van de Bruck, Mifsud & Morrice 2017; van de Bruck & Mifsud 2018; Yang et al. 2019). We here consider an interacting dark energy model in which an evolving dark energy scalar field (Peebles & Ratra 1988; Ratra & Peebles 1988; Wetterich 1988) is coupled to the dark matter quanta via the so-called conformal coupling function, and is characterized by a dark sector fifth force between the dark matter particles mediated by the dark energy scalar field. The modified cosmological evolution along with its distinct cosmological signatures on the linear and non-linear levels has been exhaustively explored in the literature (see for instance, Wetterich 1995; Amendola 2000, 2004; Farrar & Peebles 2004; Mainini & Bonometto 2006; Pettorino & Baccigalupi 2008; Baldi et al. 2010; Baldi 2011a,b, 2012a,b; van de Bruck & Morrice 2015; Odderskov et al. 2016; Mifsud & van de Bruck 2017), and tight constraints on the model parameters have been placed (Amendola & Quercellini 2003; Bean et al. 2008; Xia 2009; Amendola et al. 2012; Pettorino et al. 2012; Pettorino 2013; Xia 2013; Ade et al. 2016b; Miranda et al. 2018; van de Bruck & Mifsud 2018). Thus, the aim of our analysis is to compare the impact of the Hubble constant measurement derived from the binary neutron star system GW170817 with that of the locally inferred Hubble constant measurement on these tight model parameter constraints.

The organization of this paper is as follows. In Section 2 we briefly introduce the considered interacting dark energy model, and in Section 3 we summarize the observational data sets together with the method that will be employed to infer the cosmological parameter constraints. We then present and discuss our results in Section 4, and draw our final remarks and prospective lines of research in Section 5.

2 INTERACTING DARK ENERGY

We here briefly review the basic equations of our interacting dark energy (DE) model. The phenomenology of this dark sector interaction can be immediately grasped by writing down the Einstein frame scalar–tensor theory action:

$$S = \int d^4x\sqrt{-g}\left[\frac{M_{\rm Pl}^2}{2}R - \frac{1}{2}g^{\mu\nu}\partial_\mu\phi\,\partial_\nu\phi - V(\phi) + \mathcal{L}_{\rm SM}\right] + \int d^4x\sqrt{-\tilde{g}}\widetilde{\mathcal{L}}_{\rm DM}\left(\tilde{g}_{\mu\nu},\psi\right), \quad (1)$$

in which the gravitational sector has the standard Einstein–Hilbert form, and defines $M_{\rm Pl}^{-2} \equiv 8\pi G$ such that $M_{\rm Pl} = 2.4 \times 10^{18}$ GeV is the reduced Planck mass. DE is promoted to a dynamical scalar field, as in the vast majority of alternative DE models, and is described by a canonical quintessence scalar field ϕ, with a potential $V(\phi)$. The uncoupled SM particles are depicted by the Lagrangian $\mathcal{L}_{\rm SM}$, which incorporates a relativistic and a baryonic sector (hereafter, denoted by the subscripts r and b, respectively). Particle quanta of the dark matter (DM) fields ψ follow the geodesics defined by the metric $\tilde{g}_{\mu\nu} = C(\phi)g_{\mu\nu}$, with $C(\phi)$ being the dark sector conformal coupling function.[1]

As a consequence of the interaction between the dark sector constituents, the modified conservation equations of the energy–momentum tensors of the scalar field and DM are, respectively, given by

$$\Box\phi = V_{,\phi} - Q\,, \quad \nabla^\mu T^{\rm DM}_{\mu\nu} = Q\nabla_\nu\phi\,, \quad (2)$$

where $V_{,\phi} \equiv {\rm d}V/{\rm d}\phi$. Moreover, the dark sector coupling function is given by

$$Q = \frac{C_{,\phi}}{2C}T_{\rm DM}\,, \quad (3)$$

with $T_{\rm DM}$ being the trace of the perfect fluid energy–momentum tensor of pressureless DM, denoted by $T^{\rm DM}_{\mu\nu}$. As illustrated in equation (1), SM particles are excluded from the dark sector interaction, thus their perfect fluid energy–momentum tensor satisfies $\nabla^\mu T^{\rm SM}_{\mu\nu} = 0$.

On assuming a spatially flat Friedmann–Lemaître–Robertson–Walker (FLRW) line element, specified by ${\rm d}s^2 = g_{\mu\nu}{\rm d}x^\mu{\rm d}x^\nu = a^2(\tau)[-{\rm d}\tau^2 + \delta_{ij}{\rm d}x^i{\rm d}x^j]$, the evolution of the DE scalar field is governed by

$$\phi'' + 2\mathcal{H}\phi' + a^2V_{,\phi} = a^2Q\,, \quad (4)$$

where a prime denotes a derivative with respect to conformal time τ, and defines the conformal Hubble parameter by $\mathcal{H} = a'/a$, with $a(\tau)$ being the cosmological scale factor. Furthermore, the DM energy density, $\rho_{\rm c}$, satisfies an energy exchange equation, given by

$$\rho_{\rm c}' + 3\mathcal{H}\rho_{\rm c} = -Q\phi'\,, \quad (5)$$

where the coupling function in FLRW simplifies (Wetterich 1995; Amendola 2000; Zumalacárregui et al. 2013; van de Bruck & Morrice 2015; Mifsud & van de Bruck 2017) to $Q = -C_{,\phi}\rho_{\rm c}/(2C)$. Throughout this paper, we adopt the following exponential conformal coupling and scalar field potential functions

$$C(\phi) = e^{2\alpha\phi/M_{\rm Pl}}\,, \quad V(\phi) = V_0^4 e^{-\lambda\phi/M_{\rm Pl}}\,, \quad (6)$$

where α, V_0, and λ are constants.

[1]This metric transformation can be considered as a particular case of a generalized transformation that takes into account a conformal as well as a non-vanishing disformal (Bekenstein 1993) dark sector coupling function (Zumalacárregui, Koivisto & Mota 2013; Koivisto, Wills & Zavala 2014; van de Bruck & Morrice 2015; Mifsud & van de Bruck 2017; van de Bruck et al. 2017; van de Bruck & Mifsud 2018; Xiao et al. 2019).

Due to the non-negligible cosmological imprints on the evolution of cosmic perturbations and background dynamics, such an interaction within the dark sector has been widely studied and tight constraints were inferred from several cosmological probes (see for instance, Amendola & Quercellini 2003; Bean et al. 2008; Xia 2009; Amendola et al. 2012; Pettorino et al. 2012; Pettorino 2013; Xia 2013; Ade et al. 2016b; Miranda et al. 2018; van de Bruck & Mifsud 2018, and references therein). We here illustrate the distinctive imprints of two independent Hubble constant measurements on the *Planck* and cosmic expansion constraints, particularly on the allowed conformal coupling strength parameter values.

3 DATA SETS AND METHOD

We now discuss the data sets that are used to confront the above interacting DE model. In all data set combinations, we consider the low-multipole ($2 \leq \ell \leq 29$) publicly available *Planck* 2015 data (Aghanim et al. 2016a), along with the high-multipole ($\ell \geq 30$) range, and the *Planck* lensing likelihood in the multipole range $40 \leq \ell \leq 400$ (Ade et al. 2016c). In the following, we refer to this combination of temperature, polarization, and lensing CMB angular power spectra as '*Planck*'. We remark that the inferred parameter constraints with the temperature CMB angular power spectrum only have been shown (van de Bruck & Mifsud 2018) to be significantly weaker, albeit consistent, than those derived from the considered CMB power spectra.

In order to assess the impact of independent measurements of the Hubble constant on the inferred model parameter constraints, we make use of a local measurement of the Hubble constant (hereafter denoted by $H_0^{\rm R}$) (Riess et al. 2016) and the first gravitational-wave standard siren measurement (hereafter, denoted by $H_0^{\rm GW}$) (Abbott et al. 2017b). Since the latter marginalized posterior distribution for the Hubble constant is strongly non-Gaussian, we implemented this prior via an interpolating generalized normal distribution function that can adequately reproduce the reported constraint of Abbott et al. (2017b).

In addition, we occasionally further include information on the cosmic expansion history by making use of Hubble parameter measurements at several redshifts derived from the cosmic chronometers technique (Simon, Verde & Jimenez 2005; Stern et al. 2010; Moresco et al. 2012; Zhang et al. 2014; Moresco 2015; Moresco et al. 2016; Ratsimbazafy et al. 2017) and also from BAO surveys (Alam et al. 2017; Bautista et al. 2017; du Mas des Bourboux et al. 2017), which we, respectively, refer to as $H(z)^{\rm CC}$ and $H(z)^{\rm BAO}$.

We infer the parameter posterior distributions together with their confidence limits via a customized version of the Markov Chain Monte Carlo (MCMC) package `Monte Python` (Audren et al.

Table 1. External flat priors on the cosmological parameters assumed in this paper.

Parameter	Prior
$\Omega_{\rm b}h^2$	[0.005, 0.100]
$\Omega_{\rm c}h^2$	[0.01, 0.99]
$100\,\theta_{\rm s}$	[0.5, 10.0]
$\tau_{\rm reio}$	[0.02, 0.80]
$\ln(10^{10}A_{\rm s})$	[2.7, 4.0]
$n_{\rm s}$	[0.5, 1.5]
λ	[0.0, 1.7]
α	[0.00, 0.48]

2013), which is interfaced with a modified version of the cosmological Boltzmann code `CLASS` (Blas, Lesgourgues & Tram 2011), in which we evolve the background as well as the synchronous gauge linear perturbation equations (Mifsud & van de Bruck 2017). For our results, we also made use of the MCMC analysis package `GetDist` (Lewis & Bridle 2002), and checked that the results are in an excellent agreement with those obtained from `Monte Python`.

We consider flat priors for the interacting DE model parameters that are allowed to vary in our MCMC analyses. The full range of each flat prior is listed in Table 1, and refer the reader to our previous analyses (van de Bruck et al. 2017; van de Bruck & Mifsud 2018) for our choice of priors. This set of parameters consists of $\Theta = \left\{\Omega_b h^2,\ \Omega_c h^2,\ 100\,\theta_s,\ \tau_{\rm reio},\ \ln(10^{10}A_s),\ n_s,\ \lambda,\ \alpha\right\}$. Here, h is defined in terms of the Hubble constant via $H_0 = 100\,h$ km s^{-1} Mpc^{-1}, $\Omega_b h^2$ represents the effective fractional abundance of uncoupled baryons, $\Omega_c h^2$ is the pressureless coupled CDM effective energy density, $100\,\theta_s$ is the angular scale of the sound horizon at last scattering defined by the ratio of the sound horizon at decoupling to the angular diameter distance to the last scattering surface, $\tau_{\rm reio}$ is the reionization optical depth parameter, $\ln(10^{10}A_s)$ is the log power of the scalar amplitude of the primordial power spectrum together with its scalar spectral index n_s, λ is the slope of the scalar field exponential potential, and α is the conformal coupling parameter. The inferred constraints on these parameters are reported in the top block of Tables 2–4. Moreover, we also vary the nuisance parameters according to the procedure described in Ade et al. (2016a) and Aghanim et al. (2016a). In the lower block of Tables 2–4, we present marginalized constraints on a number of derived cosmological parameters, including H_0, the current total fractional abundance of non-relativistic matter Ω_m, the linear theory rms fluctuation in total matter in $8\,h^{-1}$ Mpc spheres denoted by σ_8, and the reionization redshift $z_{\rm reio}$. We further adopt a pivot scale of $k_0 = 0.05\,{\rm Mpc}^{-1}$, and we assume purely adiabatic scalar perturbations at very early times with null runnings of the scalar spectral index. Moreover, we fix the neutrino effective number to its standard value of $N_{\rm eff} = 3.046$ (Mangano et al. 2002), as well as the photon temperature today to $T_0 = 2.7255$ K (Fixsen 2009). As mentioned earlier, we assume spatial flatness.

4 RESULTS

We here discuss the inferred cosmological parameter constraints following the procedure described in Section 3. As illustrated in the second column of Table 2, the *Planck* data set places tight limits on all model parameters, allowing only for a tiny conformal coupling within the dark cosmic sector. This is consistent with our previous analyses that we presented in van de Bruck & Mifsud (2018), where we further showed that the inclusion of large-scale structure cosmic probes leads to tighter upper limits on α, although a mild tension exists between some of these growth-of-structure data sets in the spatially flat ΛCDM model (Henry et al. 2009; Vikhlinin et al. 2009; Mantz et al. 2010; Rozo et al. 2010; Tinker et al. 2012; Benson et al. 2013; Hajian et al. 2013; Ade et al. 2014b). Thus, the cosmological bounds presented in this analysis should be considered as complementary and conservative. If we first focus on the Hubble constant constraints reported in Table 2, we clearly observe that the *Planck* data set prefers lower values of H_0 with respect to when we consider $H_0^{\rm GW}$, and particularly when we take into account the $H_0^{\rm R}$ prior. Consequently, a slightly larger dark sector coupling is allowed when we consider the *Planck* + $H_0^{\rm GW}$ data set combination, although the inferred constraints are consistent with the *Planck* data set constraints. However, the *Planck* + $H_0^{\rm R}$ joint data set leads to a non-null dark sector coupling at a statistically high significance (see Figs 1 and 2). Due to the well-known correlation between the parameters α and σ_8 (van de Bruck & Mifsud 2018), the *Planck* + $H_0^{\rm R}$ bound on α gives rise to a significantly large value of σ_8 which might not be fully compatible with probes of the large-scale structure (see van de Bruck & Mifsud 2018, for a detailed discussion).

Since the CMB anisotropies mainly probe the high-redshift Universe, we further add some information about the low-redshift cosmic expansion by considering the $H(z)^{\rm CC}$ and $H(z)^{\rm BAO}$ data sets, as described in Section 3. We present these constraints in Table 3, where we independently consider the $H(z)^{\rm CC}$ and $H(z)^{\rm BAO}$ data sets along with the *Planck* data set and the Hubble constant priors, whereas in Table 4 we jointly consider the Hubble parameter measurements [hereafter, denoted by $H(z)^{\rm CC+BAO}$]. The consideration of these cosmic expansion measurements leads to improved constraints on the interacting DE model parameters with respect to the inferred constraints from the *Planck* data set only. As we clearly illustrate in Figs 1 and 2, the $H_0^{\rm GW}$ prior always gives consistent constraints on α with those derived from the *Planck* + $H(z)^{\rm CC}$, *Planck* + $H(z)^{\rm BAO}$, and *Planck* + $H(z)^{\rm CC+BAO}$ data set combinations. On the other hand, the $H_0^{\rm R}$ prior is always found to be associated with a non-null conformal coupling between DM and DE, although the inclusion of the cosmic expansion data sets leads to slightly smaller values of α with respect to the *Planck* only constraints, but still not consistent with a vanishing dark sector coupling.

Moreover, the H_0 likelihood priors improve the upper limit on the scalar field exponential potential parameter λ, particularly when we consider the $H_0^{\rm R}$ measurement in our data set combinations. This is depicted in Fig. 3, where we show the two-dimensional posteriors for the *Planck* + $H(z)^{\rm CC+BAO}$, *Planck* + $H(z)^{\rm CC+BAO}$ + $H_0^{\rm GW}$, and *Planck* + $H(z)^{\rm CC+BAO}$ + $H_0^{\rm R}$ data sets in the λ–α plane, along with colour-coded samples depicting the value of the Hubble constant. In Fig. 4 we show the marginal correlation between α and H_0 (consistent with van de Bruck & Mifsud 2018), where we present the two-dimensional likelihood constraints in the H_0–α plane. From Figs 3 and 4, we can clearly see the consistency between the inferred constraints in the λ–α and H_0–α planes with the *Planck* + $H(z)^{\rm CC+BAO}$ and *Planck* + $H(z)^{\rm CC+BAO}$ + $H_0^{\rm GW}$ joint data sets. Since the cosmic distance ladder measurement of the Hubble constant is more accurate than the gravitational-wave standard siren measurement, such that the latter is compatible with a broad range of H_0 values, it is expected that tighter constraints on H_0 are derived in our interacting DE model when we make use of the $H_0^{\rm R}$ likelihood prior. This is depicted in Fig. 4, where we also observe the preference for a non-null interaction in the dark cosmic sector. Unequivocally, independent constraints on the Hubble constant would be able to shed light on the nature of DE and DM, and provide complementary constraints to the forthcoming cosmological surveys, which are forecasted (Amendola et al. 2012; Casas et al. 2016; Miranda et al. 2018) to place very tight limits on this dark sector interaction.

5 CONCLUSIONS

We quantitatively examined the impact of independent Hubble constant measurements on a tightly constrained direct coupling between DM and DE. In our interacting DE model, we specifically considered a conformal coupling within the dark cosmic sector, in

Table 2. For each model parameter, we report the mean values and 1σ errors, together with the 1σ (2σ) upper limits of λ and α. The Hubble constant is given in units of km s^{-1} Mpc^{-1}.

Parameter	*Planck*	$+H_0^{\rm GW}$	$+H_0^{\rm R}$
$100\,\Omega_{\rm b}h^2$	$2.2261^{+0.0166}_{-0.0172}$	$2.2263^{+0.0163}_{-0.0168}$	$2.2274^{+0.0168}_{-0.0171}$
$\Omega_{\rm c}h^2$	$0.11747^{+0.00335}_{-0.00185}$	$0.11735^{+0.00342}_{-0.00175}$	$0.11356^{+0.00240}_{-0.00245}$
$100\,\theta_{\rm s}$	$1.04180^{+0.00032}_{-0.00033}$	$1.04180^{+0.00032}_{-0.00032}$	$1.04190^{+0.00032}_{-0.00032}$
$\tau_{\rm reio}$	$0.0636^{+0.0142}_{-0.0145}$	$0.0634^{+0.0140}_{-0.0143}$	$0.0662^{+0.0139}_{-0.0140}$
$\ln(10^{10}A_{\rm s})$	$3.0600^{+0.0267}_{-0.0263}$	$3.0596^{+0.0258}_{-0.0263}$	$3.0650^{+0.0254}_{-0.0262}$
$n_{\rm s}$	$0.96651^{+0.00506}_{-0.00539}$	$0.96658^{+0.00502}_{-0.00529}$	$0.96906^{+0.00481}_{-0.00512}$
λ	$0.815^{+0.291}_{-0.815}$	$0.774^{+0.263}_{-0.774}$	$0.523^{+0.156}_{-0.523}$
α	$0.0408^{+0.0122}_{-0.0408}$	$0.0416^{+0.0126}_{-0.0416}$	$0.0718^{+0.0208}_{-0.0169}$
λ	$<1.1062(1.6001)$	$<1.0370(1.5686)$	$<0.6785(1.1979)$
α	$<0.0529(0.0912)$	$<0.0542(0.0921)$	$<0.0925(0.1132)$
H_0	$67.90^{+2.80}_{-3.22}$	$68.18^{+2.70}_{-3.00}$	$72.04^{+1.82}_{-1.86}$
$\Omega_{\rm m}$	$0.3053^{+0.0321}_{-0.0316}$	$0.3024^{+0.0314}_{-0.0284}$	$0.2624^{+0.0167}_{-0.0187}$
σ_8	$0.8301^{+0.0264}_{-0.0360}$	$0.8326^{+0.0247}_{-0.0368}$	$0.8738^{+0.0240}_{-0.0246}$
$z_{\rm reio}$	$8.54^{+1.42}_{-1.29}$	$8.52^{+1.41}_{-1.26}$	$8.74^{+1.38}_{-1.21}$

Table 3. As in Table 2, we here report the mean values and 1σ errors for each model parameter, together with the 1σ (2σ) upper limits of λ and α. The Hubble constant is given in units of km s^{-1} Mpc^{-1}.

Parameter	*Planck* $+H(z)^{\rm CC}$	$+H_0^{\rm GW}$	$+H_0^{\rm R}$	*Planck* $+H(z)^{\rm BAO}$	$+H_0^{\rm GW}$	$+H_0^{\rm R}$
$100\,\Omega_{\rm b}h^2$	$2.2260^{+0.0164}_{-0.0166}$	$2.2265^{+0.0159}_{-0.0166}$	$2.2280^{+0.0172}_{-0.0171}$	$2.2267^{+0.0163}_{-0.0167}$	$2.2265^{+0.0166}_{-0.0167}$	$2.2275^{+0.0168}_{-0.0172}$
$\Omega_{\rm c}h^2$	$0.11823^{+0.00226}_{-0.00169}$	$0.11812^{+0.00226}_{-0.00170}$	$0.11504^{+0.00206}_{-0.00203}$	$0.11813^{+0.00231}_{-0.00165}$	$0.11796^{+0.00237}_{-0.00167}$	$0.11471^{+0.00205}_{-0.00199}$
$100\,\theta_{\rm s}$	$1.04180^{+0.00031}_{-0.00032}$	$1.04180^{+0.00032}_{-0.00032}$	$1.04190^{+0.00032}_{-0.00032}$	$1.04180^{+0.00031}_{-0.00031}$	$1.04180^{+0.00032}_{-0.00032}$	$1.04180^{+0.00032}_{-0.00032}$
$\tau_{\rm reio}$	$0.0627^{+0.0138}_{-0.0141}$	$0.0629^{+0.0139}_{-0.0142}$	$0.0655^{+0.0140}_{-0.0141}$	$0.0631^{+0.0139}_{-0.0139}$	$0.0631^{+0.0140}_{-0.0141}$	$0.0649^{+0.0139}_{-0.0141}$
$\ln(10^{10}A_{\rm s})$	$3.0580^{+0.0257}_{-0.0257}$	$3.0585^{+0.0262}_{-0.0259}$	$3.0632^{+0.0256}_{-0.0259}$	$3.0590^{+0.0258}_{-0.0257}$	$3.0589^{+0.0255}_{-0.0259}$	$3.0624^{+0.0260}_{-0.0256}$
n_s	$0.96589^{+0.00486}_{-0.00506}$	$0.96605^{+0.00485}_{-0.00511}$	$0.96806^{+0.00477}_{-0.00490}$	$0.96616^{+0.00486}_{-0.00495}$	$0.96621^{+0.00487}_{-0.00497}$	$0.96794^{+0.00474}_{-0.00489}$
λ	$0.770^{+0.263}_{-0.770}$	$0.729^{+0.241}_{-0.729}$	$0.415^{+0.120}_{-0.415}$	$0.845^{+0.537}_{-0.592}$	$0.785^{+0.271}_{-0.785}$	$0.415^{+0.123}_{-0.415}$
α	$0.0338^{+0.0104}_{-0.0338}$	$0.0342^{+0.0107}_{-0.0342}$	$0.0589^{+0.0209}_{-0.0139}$	$0.0354^{+0.0144}_{-0.0319}$	$0.0365^{+0.0170}_{-0.0308}$	$0.0623^{+0.0194}_{-0.0125}$
λ	$<1.0329(1.5707)$	$<0.9698(1.5203)$	$<0.5350(0.9883)$	$<1.3825(1.6113)$	$<1.0559(1.5703)$	$<0.5386(0.9587)$
α	$<0.0443(0.0723)$	$<0.0448(0.0724)$	$<0.0798(0.0933)$	$<0.0498(0.0733)$	$<0.0535(0.0742)$	$<0.0816(0.0950)$
H_0	$67.45^{+2.53}_{-2.06}$	$67.68^{+2.34}_{-1.93}$	$70.99^{+1.55}_{-1.60}$	$67.25^{+2.88}_{-2.48}$	$67.61^{+2.67}_{-2.32}$	$71.31^{+1.58}_{-1.59}$
$\Omega_{\rm m}$	$0.3101^{+0.0201}_{-0.0274}$	$0.3075^{+0.0204}_{-0.0248}$	$0.2729^{+0.0154}_{-0.0164}$	$0.3121^{+0.0248}_{-0.0315}$	$0.3082^{+0.0230}_{-0.0291}$	$0.2699^{+0.0149}_{-0.0164}$
σ_8	$0.8242^{+0.0245}_{-0.0237}$	$0.8263^{+0.0230}_{-0.0227}$	$0.8604^{+0.0206}_{-0.0216}$	$0.8225^{+0.0267}_{-0.0278}$	$0.8260^{+0.0257}_{-0.0269}$	$0.8641^{+0.0213}_{-0.0216}$
$z_{\rm reio}$	$8.46^{+1.42}_{-1.25}$	$8.48^{+1.42}_{-1.26}$	$8.69^{+1.39}_{-1.24}$	$8.51^{+1.41}_{-1.23}$	$8.50^{+1.42}_{-1.24}$	$8.64^{+1.39}_{-1.23}$

which DE is described by a dynamical canonical scalar field and the gravitational attraction between the DM particles deviates from the standard one in General Relativity, such that the effective attraction is enhanced by the presence of a fifth force. Since this coupling has been repeatedly shown to be robustly constrained by the *Planck* CMB data set (see for instance, Pettorino 2013; Xia 2013; Ade et al. 2016b; Miranda et al. 2018; van de Bruck & Mifsud 2018), we have always considered this crucial information in our joint data sets. Indeed, tight limits on all model parameters have been placed solely with the *Planck* data set, including tight upper limits on the conformal coupling strength parameter α, and the slope of the scalar field exponential potential λ. Moreover, we showed that the inclusion of a number of Hubble parameter measurements improves the *Planck*-only constraints.

In all our analyses that further considered the gravitational-wave standard siren measurement of the Hubble constant $H_0^{\rm GW}$, we found that this likelihood prior is compatible with a slightly larger conformal coupling within the dark cosmic sector, and marginally improves the upper limits on λ. Thus, we expect that near-future standard siren measurements of the Hubble constant would place tighter constraints on this interacting DE model. Furthermore, this Hubble constant prior was not found to shift the model parameter constraints inferred from the more established cosmological data sets, and could therefore be considered as a conservative likelihood prior.

On the other hand, the inclusion of the more precise measurement of the Hubble constant derived from observations of Cepheid variables (Riess et al. 2016) was always found to be characterized by a non-null interaction between DM and DE in the framework of the considered interacting DE model, as it can be seen from the blue region in Fig. 4. Although our results indicate that there is a strong preference for a non-vanishing dark sector coupling for this choice of data, it is important to notice that there are several precise cosmological data sets that can provide much

Table 4. As in Tables 2 and 3, we here report the mean values and 1σ errors for each model parameter, together with the 1σ (2σ) upper limits of λ and α. The Hubble constant is given in units of km s^{-1} Mpc^{-1}.

Parameter	$Planck + H(z)^{\rm CC+BAO}$	$+H_0^{\rm GW}$	$+H_0^{\rm R}$
$100\ \Omega_{\rm b}h^2$	$2.2267^{+0.0162}_{-0.0168}$	$2.2267^{+0.0162}_{-0.0167}$	$2.2280^{+0.0167}_{-0.0174}$
$\Omega_{\rm c}h^2$	$0.11830^{+0.00191}_{-0.00160}$	$0.11819^{+0.00193}_{-0.00160}$	$0.11554^{+0.00187}_{-0.00182}$
$100\ \theta_{\rm s}$	$1.04180^{+0.00032}_{-0.00032}$	$1.04180^{+0.00032}_{-0.00031}$	$1.04190^{+0.00031}_{-0.00032}$
$\tau_{\rm reio}$	$0.0631^{+0.0138}_{-0.0141}$	$0.0630^{+0.0138}_{-0.0142}$	$0.0647^{+0.0138}_{-0.0143}$
$\ln(10^{10}A_{\rm s})$	$3.0589^{+0.0254}_{-0.0259}$	$3.0585^{+0.0258}_{-0.0257}$	$3.0617^{+0.0259}_{-0.0258}$
$n_{\rm s}$	$0.96599^{+0.00476}_{-0.00490}$	$0.96601^{+0.00471}_{-0.00490}$	$0.96752^{+0.00471}_{-0.00486}$
λ	$0.802^{+0.315}_{-0.762}$	$0.744^{+0.250}_{-0.744}$	$0.386^{+0.113}_{-0.386}$
α	$0.0334^{+0.0170}_{-0.0261}$	$0.0342^{+0.0182}_{-0.0248}$	$0.0551^{+0.0201}_{-0.0121}$
λ	$<1.1164(1.5774)$	$<0.9940(1.5273)$	$<0.4985(0.9075)$
α	$<0.0504(0.0675)$	$<0.0524(0.0680)$	$<0.0753(0.0874)$
H_0	$67.27^{+2.64}_{-1.97}$	$67.58^{+2.42}_{-1.75}$	$70.66^{+1.40}_{-1.42}$
$\Omega_{\rm m}$	$0.3118^{+0.0202}_{-0.0279}$	$0.3085^{+0.0189}_{-0.0247}$	$0.2764^{+0.0141}_{-0.0148}$
σ_8	$0.8224^{+0.0250}_{-0.0227}$	$0.8252^{+0.0232}_{-0.0216}$	$0.8565^{+0.0192}_{-0.0203}$
$z_{\rm reio}$	$8.51^{+1.40}_{-1.25}$	$8.49^{+1.40}_{-1.26}$	$8.62^{+1.39}_{-1.26}$

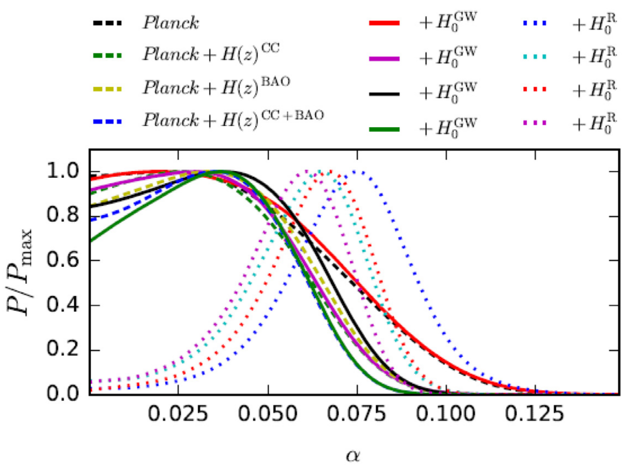

Figure 1. Marginalized one-dimensional posterior distributions for the conformal coupling parameter α, with the different data set combinations indicated in the figure. The respective parameter constraints are tabulated in Tables 2–4.

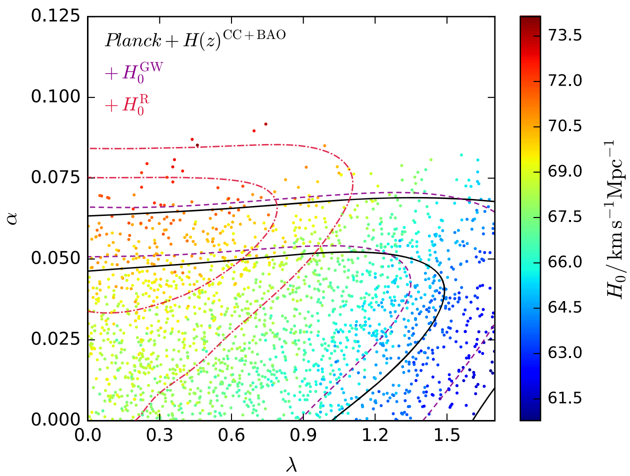

Figure 3. Marginalized two-dimensional constraints on the parameters λ and α, together with samples from the $Planck + H(z)^{\rm CC+BAO}$ joint data set colour coded with the value of the Hubble constant.

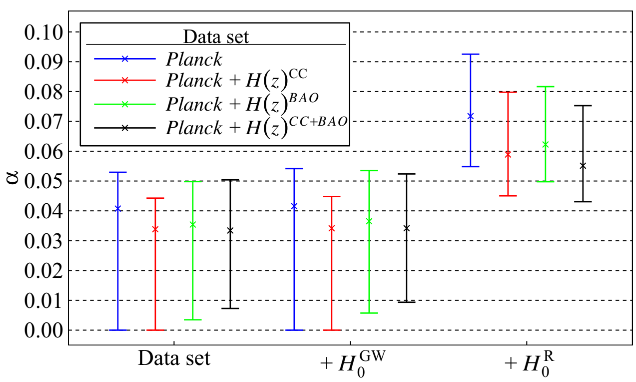

Figure 2. The coloured intervals correspond to the inferred 1σ two-tail limits on the conformal coupling strength parameter α. We illustrate all the data set combinations considered in this paper.

tighter constraints on the model parameters and presumably not compatible with such a large coupling (Miranda et al. 2018; van de Bruck & Mifsud 2018). Having said that, other independent Hubble constant measurements, such as from the time-delay distances in gravitationally lensed quasar systems (Bonvin et al. 2017; Birrer et al. 2019), have been shown to be in agreement with the cosmic distance ladder measurement in the framework of the concordance model of cosmology. Thus, prospective data from CMB experiments and galaxy surveys, along with more observations of standard sirens that would be able to improve current estimates on the Hubble constant, will certainly enhance our understanding of the dark cosmic sector and potentially resolve the several tensions present between a number of cosmological probes.

NOTE ADDED

While this paper was being written up, a new constraint on the Hubble constant was presented in Soares-Santos et al. (2019), from

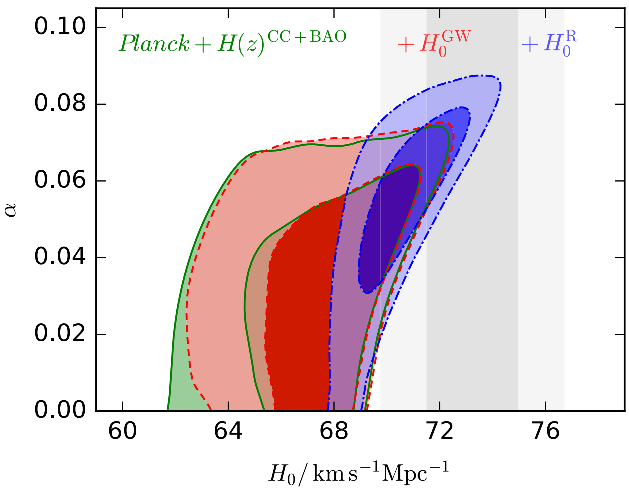

Figure 4. Marginalized two-dimensional likelihood constraints on the Hubble constant and the conformal coupling parameter α with different data set combinations indicated in the figure. The grey (light grey) band shows the 1σ (2σ) constraint on the Hubble constant as reported in Riess et al. (2016).

another gravitational-wave source, the binary black-hole merger GW170814. The value stated, $H_0 = 75.2^{+39.5}_{-32.4}$ km s^{-1} Mpc^{-1}, has larger error bars than the one used in our analyses. Because of this, adding this supplementary observation will not alter the results presented in the paper here. But clearly the future is bright for multimessenger astronomy.

ACKNOWLEDGEMENTS

The work of CvdB is supported by the Lancaster–Manchester–Sheffield Consortium for Fundamental Physics under STFC Grant No. ST/L000520/1.

REFERENCES

Abazajian K. N. et al., 2016, preprint (arXiv:1610.02743)
Abbott B. et al., 2017a, Phys. Rev. Lett., 119, 161101
Abbott B. P. et al., 2017b, Nature, 551, 85
Abbott B. P. et al., 2017c, ApJ, 848, L12
Abbott B. P. et al., 2017d, ApJ, 848, L13
Abbott B. P. et al., 2018, preprint (arXiv:1811.00364)
Addison G. E., Huang Y., Watts D. J., Bennett C. L., Halpern M., Hinshaw G., Weiland J. L., 2016, ApJ, 818, 132
Ade P. A. R. et al., 2014a, A&A, 571, A16
Ade P. A. R. et al., 2014b, A&A, 571, A20
Ade P. A. R. et al., 2016a, A&A, 594, A13
Ade P. A. R. et al., 2016b, A&A, 594, A14
Ade P. A. R. et al., 2016c, A&A, 594, A15
Aghanim N. et al., 2016a, A&A, 594, A11
Aghanim N. et al., 2016b, A&A, 596, A107
Aghanim N. et al., 2018, preprint (arXiv:1807.06209)
Alam S. et al., 2017, MNRAS, 470, 2617
Amendola L., 2000, Phys. Rev. D, 62, 043511
Amendola L., 2004, Phys. Rev. D, 69, 103524
Amendola L., Quercellini C., 2003, Phys. Rev. D, 68, 023514
Amendola L., Pettorino V., Quercellini C., Vollmer A., 2012, Phys. Rev. D, 85, 103008
Arcavi I. et al., 2017, Nature, 551, 64
Archidiacono M., Gariazzo S., Giunti C., Hannestad S., Hansen R., Laveder M., Tram T., 2016, J. Cosmol. Astropart. Phys., 2016, 067
Audren B., Lesgourgues J., Benabed K., Prunet S., 2013, J. Cosmol. Astropart. Phys., 1302, 001
Baker T., Bellini E., Ferreira P. G., Lagos M., Noller J., Sawicki I., 2017, Phys. Rev. Lett., 119, 251301
Baldi M., 2011a, MNRAS, 411, 1077
Baldi M., 2011b, MNRAS, 414, 116
Baldi M., 2012a, MNRAS, 420, 430
Baldi M., 2012b, MNRAS, 422, 1028
Baldi M., Pettorino V., Robbers G., Springel V., 2010, MNRAS, 403, 1684
Bautista J. E. et al., 2017, A&A, 603, A12
Bean R., Flanagan E. E., Laszlo I., Trodden M., 2008, Phys. Rev. D, 78, 123514
Bekenstein J. D., 1993, Phys. Rev. D, 48, 3641
Belgacem E., Dirian Y., Foffa S., Maggiore M., 2018, Phys. Rev. D, 98, 023510
Benetti M., Graef L. L., Alcaniz J. S., 2018, J. Cosmol. Astropart. Phys., 2018, 066
Benson B. A. et al., 2013, ApJ, 763, 147
Bernal J. L., Verde L., Riess A. G., 2016, J. Cosmol. Astropart. Phys., 2016, 019
Bertotti B., Iess L., Tortora P., 2003, Nature, 425, 374
Birrer S. et al., 2019, MNRAS, 484, 4726
Blas D., Lesgourgues J., Tram T., 2011, J. Cosmol. Astropart. Phys., 1107, 034
Bonvin V. et al., 2017, MNRAS, 465, 4914
Cahillane C. et al., 2017, Phys. Rev. D, 96, 102001
Camarena D., Marra V., 2018, Phys. Rev. D, 98, 023537
Cardona W., Kunz M., Pettorino V., 2017, J. Cosmol. Astropart. Phys., 2017, 056
Carroll S. M., 1998, Phys. Rev. Lett., 81, 3067
Carroll S. M., Mantry S., Ramsey-Musolf M. J., Stubbs C. W., 2009, Phys. Rev. Lett., 103, 011301
Casas S., Amendola L., Baldi M., Pettorino V., Vollmer A., 2016, J. Cosmol. Astropart. Phys., 2016, 045
Chen H.-Y., Fishbach M., Holz D. E., 2018, Nature, 562, 545
Chernoff D. F., Finn L. S., 1993, ApJ, 411, L5
Colgáin E. O., Van Putten M. H. P. M., Yavartanoo H., 2018, preprint (arXiv:1807.07451)
Congedo G., 2017, Int. J. Mod. Phys. D, 26, 1741022
Congedo G., Taylor A., 2019, Phys. Rev. D, 99, 083526
Coulter D. A. et al., 2017, Science, 358, 1556
Creminelli P., Vernizzi F., 2017, Phys. Rev. Lett., 119, 251302
Cutler C., Holz D. E., 2009, Phys. Rev. D, 80, 104009
Dalal N., Holz D. E., Hughes S. A., Jain B., 2006, Phys. Rev. D, 74, 063006
Damour T., Gibbons G. W., Gundlach C., 1990, Phys. Rev. Lett., 64, 123
Davis D., Massinger T. J., Lundgren A. P., Driggers J. C., Urban A. L., Nuttall L. K., 2019, Class. Quantum Gravity, 36, 055011
de Rham C., Melville S., 2018, Phys. Rev. Lett., 121, 221101
Del Pozzo W., 2012, Phys. Rev. D, 86, 043011
Dhawan S., Jha S. W., Leibundgut B., 2018, A&A, 609, A72
Dima A., Vernizzi F., 2018, Phys. Rev. D, 97, 101302
Di Valentino E. et al., 2018d, J. Cosmol. Astropart. Phys., 1804, 017
Di Valentino E., Melchiorri A., 2018, Phys. Rev. D, 97, 041301
Di Valentino E., Melchiorri A., Silk J., 2016, Phys. Lett. B, 761, 242
Di Valentino E., Melchiorri A., Linder E. V., Silk J., 2017a, Phys. Rev. D, 96, 023523
Di Valentino E., Melchiorri A., Mena O., 2017b, Phys. Rev. D, 96, 043503
Di Valentino E., Bøehm C., Hivon E., Bouchet F. R., 2018a, Phys. Rev. D, 97, 043513
Di Valentino E., Linder E. V., Melchiorri A., 2018b, Phys. Rev. D, 97, 043528
Di Valentino E., Holz D. E., Melchiorri A., Renzi F., 2018c, Phys. Rev. D, 98, 083523
du Mas des Bourboux H. et al., 2017, A&A, 608, A130
Ezquiaga J. M., Zumalacárregui M., 2017, Phys. Rev. Lett., 119, 251304
Farrar G. R., Peebles P. J. E., 2004, ApJ, 604, 1
Feeney S. M., Peiris H. V., Williamson A. R., Nissanke S. M., Mortlock D. J., Alsing J., Scolnic D., 2018a, Phys. Rev. Lett., 122, 061105

Feeney S. M., Mortlock D. J., Dalmasso N., 2018b, MNRAS, 476, 3861
Ferreira E. G. M., Quintin J., Costa A. A., Abdalla E., Wang B., 2017, Phys. Rev. D, 95, 043520
Finn L. S., 1996, Phys. Rev. D, 53, 2878
Fixsen D. J., 2009, ApJ, 707, 916
Follin B., Knox L., 2018, MNRAS, 477, 4534
Goldstein A. et al., 2017, ApJ, 848, L14
Grandis S., Rapetti D., Saro A., Mohr J. J., Dietrich J. P., 2016, MNRAS, 463, 1416
Gubser S. S., Peebles P. J. E., 2004, Phys. Rev. D, 70, 123511
Hajian A., Battaglia N., Spergel D. N., Richard Bond J., Pfrommer C., Sievers J. L., 2013, J. Cosmol. Astropart. Phys., 1311, 064
Henry J. P., Evrard A. E., Hoekstra H., Babul A., Mahdavi A., 2009, ApJ, 691, 1307
Holden D. J., Wands D., 2000, Phys. Rev. D, 61, 043506
Holz D. E., Hughes S. A., 2005, ApJ, 629, 15
Hotokezaka K., Nakar E., Gottlieb O., Nissanke S., Masuda K., Hallinan G., Mooley K. P., Deller A., 2018, preprint (arXiv:1806.10596)
Huang Q.-G., Wang K., 2016, Eur. Phys. J. C, 76, 506
Karki S. et al., 2016, Rev. Sci. Instrum., 87, 114503
Karwal T., Kamionkowski M., 2016, Phys. Rev. D, 94, 103523
Ko P., Tang Y., 2016, Phys. Lett. B, 762, 462
Koivisto T., Wills D., Zavala I., 2014, J. Cosmol. Astropart. Phys., 2014, 036
Krolak A., Schutz B. F., 1987, Gen. Relativ. Gravit., 19, 1163
Kumar S., Nunes R. C., 2016, Phys. Rev. D, 94, 123511
Kumar S., Nunes R. C., 2017, Phys. Rev. D, 96, 103511
Lancaster L., Cyr-Racine F.-Y., Knox L., Pan Z., 2017, J. Cosmol. Astropart. Phys., 2017, 033
Langlois D., Saito R., Yamauchi D., Noui K., 2018, Phys. Rev. D, 97, 061501
Lewis A., Bridle S., 2002, Phys. Rev. D, 66, 103511
Lombriser L., Taylor A., 2016, J. Cosmol. Astropart. Phys., 2016, 031
MacLeod C. L., Hogan C. J., 2008, Phys. Rev. D, 77, 043512
Mainini R., Bonometto S., 2006, Phys. Rev. D, 74, 043504
Mangano G., Miele G., Pastor S., Peloso M., 2002, Phys. Lett. B, 534, 8
Mantz A., Allen S. W., Rapetti D., Ebeling H., 2010, MNRAS, 406, 1759
Marković D., 1993, Phys. Rev. D, 48, 4738
Mifsud J., van de Bruck C., 2017, J. Cosmol. Astropart. Phys., 2017, 001
Miranda V., Carrillo Gonzalez M., Krause E., Trodden M., 2018, Phys. Rev. D, 97, 063511
Moresco M. et al., 2012, J. Cosmol. Astropart. Phys., 1208, 006
Moresco M. et al., 2016, J. Cosmol. Astropart. Phys., 1605, 014
Moresco M., 2015, MNRAS, 450, L16
Nishizawa A., Yagi K., Taruya A., Tanaka T., 2012, Phys. Rev. D, 85, 044047
Nissanke S., Holz D. E., Dalal N., Hughes S. A., Sievers J. L., Hirata C. M., 2013, preprint (arXiv:1307.2638)
Odderskov I., Baldi M., Amendola L., 2016, J. Cosmol. Astropart. Phys., 2016, 035
Odderskov I., Hannestad S., Brandbyge J., 2017, J. Cosmol. Astropart. Phys., 2017, 022
Peebles P. J. E., Ratra B., 1988, ApJ, 325, L17
Pettorino V., 2013, Phys. Rev. D, 88, 063519
Pettorino V., Baccigalupi C., 2008, Phys. Rev. D, 77, 103003
Pettorino V., Amendola L., Baccigalupi C., Quercellini C., 2012, Phys. Rev. D, 86, 103507
Poulin V., Boddy K. K., Bird S., Kamionkowski M., 2018, Phys. Rev. D, 97, 123504
Prilepina V., Tsai Y., 2017, J. High Energy Phys., 2017, 33
Ratra B., Peebles P. J. E., 1988, Phys. Rev. D, 37, 3406
Ratsimbazafy A. L., Loubser S. I., Crawford S. M., Cress C. M., Bassett B. A., Nichol R. C., Väisänen P., 2017, MNRAS, 467, 3239
Riess A. G. et al., 2016, ApJ, 826, 56
Riess A. G. et al., 2018a, ApJ, 855, 136
Riess A. G. et al., 2018b, ApJ, 861, 126
Rozo E. et al., 2010, ApJ, 708, 645
Sakstein J., Jain B., 2017, Phys. Rev. Lett., 119, 251303
Salvatelli V., Said N., Bruni M., Melchiorri A., Wands D., 2014, Phys. Rev. Lett., 113, 181301
Sathyaprakash B. S., Schutz B. F., Van Den Broeck C., 2010, Class. Quantum Gravity, 27, 215006
Savchenko V. et al., 2017, ApJ, 848, L15
Schutz B. F., 1986, Nature, 323, 310
Simon J., Verde L., Jimenez R., 2005, Phys. Rev. D, 71, 123001
Soares-Santos M. et al., 2017, ApJ, 848, L16
Soares-Santos M. et al., 2019, ApJ, 876, L7
Solà J., Gómez-Valent A., de Cruz Pérez J., 2017, Phys. Lett. B, 774, 317
Stern D., Jimenez R., Verde L., Kamionkowski M., Stanford S. A., 2010, J. Cosmol. Astropart. Phys., 1002, 008
Tamanini N., Caprini C., Barausse E., Sesana A., Klein A., Petiteau A., 2016, J. Cosmol. Astropart. Phys., 2016, 002
Tanvir N. R. et al., 2017, ApJ, 848, L27
Taylor S. R., Gair J. R., 2012, Phys. Rev. D, 86, 023502
Taylor S. R., Gair J. R., Mandel I., 2012, Phys. Rev. D, 85, 023535
Thorne K. S., 1997, preprint (arXiv:gr-qc/9704042)
Tinker J. L. et al., 2012, ApJ, 745, 16
Valenti S. et al., 2017, ApJ, 848, L24
van de Bruck C., Mifsud J., 2018, Phys. Rev. D, 97, 023506
van de Bruck C., Morrice J., 2015, J. Cosmol. Astropart. Phys., 2015, 036
van de Bruck C., Mifsud J., Morrice J., 2017, Phys. Rev. D, 95, 043513
Vikhlinin A. et al., 2009, ApJ, 692, 1060
Wang Y., Turner E. L., 1997, Phys. Rev. D, 56, 724
Wetterich C., 1988, Nucl. Phys. B, 302, 668
Wetterich C., 1995, A&A, 301, 321
Will C. M., 2014, Living Rev. Relativ., 17, 4
Wu H.-Y., Huterer D., 2017, MNRAS, 471, 4946
Xia J.-Q., 2009, Phys. Rev. D, 80, 103514
Xia J.-Q., 2013, J. Cosmol. Astropart. Phys., 1311, 022
Xiao L.-F., An R., Zhang L., Yue B., Xu Y., Wang B., 2019, Phys. Rev. D, 99, 023528
Yang W., Nunes R. C., Pan S., Mota D. F., 2017, Phys. Rev. D, 95, 103522
Yang W., Pan S., Di Valentino E., Nunes R. C., Vagnozzi S., Mota D. F., 2018, J. Cosmol. Astropart. Phys., 2018, 019
Yang W., Pan S., Xu L., Mota D. F., 2019, MNRAS, 482, 1858
Zhang C., Zhang H., Yuan S., Zhang T.-J., Sun Y.-C., 2014, Res. Astron. Astrophys., 14, 1221
Zhang B. R., Childress M. J., Davis T. M., Karpenka N. V., Lidman C., Schmidt B. P., Smith M., 2017, MNRAS, 471, 2254
Zhao W., van den Broeck C., Baskaran D., Li T. G. F., 2011, Phys. Rev. D, 83, 023005
Zhao G.-B. et al., 2017a, Nat. Astron., 1, 627
Zhao M.-M., He D.-Z., Zhang J.-F., Zhang X., 2017b, Phys. Rev. D, 96, 043520
Zhu Z.-H., Fujimoto M.-K., Tatsumi D., 2001, A&A, 372, 377
Zumalacárregui M., Koivisto T. S., Mota D. F., 2013, Phys. Rev. D, 87, 083010

This paper has been typeset from a TEX/LATEX file prepared by the author.